Chapter 5

“Cactus” top-decorated aligned carbon nanotubes

5.1 Introduction

Since their discovery in 1991, carbon nanotubes (CNTs) have attracted great interest due to their outstanding structural, electrical and mechanical properties [1-3]. CNTs with different morphologies [4-6] have been reported by using different synthesis methods. Among them, plasma-enhanced chemical vapor deposition (PECVD) [7, 8] is a commonly used technique for the synthesis of aligned carbon nanotube array films on a substrate that is coated with a catalyst metal thin film. The growth process involves the dissociation of hydrocarbon molecules on the metal nanoparticle surface, the dissolution and saturation of carbon atoms in the catalytic particles, and the precipitation from the particles [2]. Generally, the metal film is pretreated by ammonia or hydrogen gas in order to form catalytic particles in nanometer size, which produce effective catalysts for the nanotube growth. The size of these particles is related to the diameter of CNTs. A previous study showed that carbon nanotubes could not be grown, using a recipe whereby C_2H_2 was introduced first, followed by NH_3 via plasma enhanced hot filament chemical vapor deposition (PE-HF-CVD) method [7]. Amorphous carbon produced in the C_2H_2 plasma coated on the catalyst surface and inhibited the catalytic role of catalyst particles [7]. Recently, it was found that multi-walled carbon nanotubes (MWNTs) can be grown with pure C_2H_2 by thermal CVD method with H_2/N_2 mixed gas pretreatment [9]. However, the density of the as-grown MWNTs is low, and the length is shorter compared with those grown with C_2H_2/H_2, C_2H_2/Ar, or C_2H_2/N_2 mixture gas.

Here we report “cactus” top-decorated aligned carbon nanotubes grown without NH_3 or H_2 gas pretreatment by the PECVD method. It is found that C_2H_2 gas not only acts as a carbon source but also activates the catalysts for nanotube growth under the plasma. The “cactus” morphology appears only on the top part of nanotubes while the lower body of the nanotubes retains the multi-walled structure. Surface wettability of such kind of “cactus” decorated CNTs were studied. The purpose here is to investigate the effect of surface nanostructures on surface wettability.

5.2 Experimental

In this work, “cactus” nanotubes were grown in a rf (13.56 MHz) plasma-enhanced chemical vapor deposition (PECVD) system. An iron film with a thickness in the range 5-100 nm was deposited on the silicon/quartz substrate by rf magnetron sputtering. The iron coated substrates were heated up to 700^{o}C gradually at a base pressure of 10^{-6} Torr. After that, C_2H_2 gas (15 sccm) was then introduced into the PECVD system. The working pressure and rf power were maintained at 60 mTorr and 100 W, respectively. In this same PECVD system, normal multi-walled carbon nanotubes are grown by using the same PECVD under a mixed reactant gas flow (C_2H_2/NH_3, 15sccm/30sccm) at around 700^{o}C for 1h. Scanning electron microscopy (SEM JEOL JSM-6400F), high-resolution transmission electron microscopy (HRTEM, JEOL JEM-2010F operated at 200kV), and Micro-Raman spectroscopy (Jobin Yvon T64000 system; Ar ion laser with wavelength of 514.5nm) were used to study the formation of “cactus” decorated aligned nanotubes. X-ray photoelectron spectroscopy (XPS) measurements were performed at the soft X-ray beamline at the Singapore Synchrotron Light Source (SSLS) [10]. The energy of the incident X-rays used is 700 eV. To evaluate the third

order nonlinearities as well as the relaxation dynamics of these MWCNTs on quartz, open aperture and close aperture Z scan as well as the degenerate pump probe experiments were performed at 780 nm. The laser pulses have 220 fs full width at half maximum (FWHM) temporal pulse width and 1 kHz repetition rate generated by a Ti: sapphire regenerate amplifier (Quantronix, Tian) which is seeded by a mode locked Ti: sapphire regenerate laser (Quantronix, IMRA).

5.3 Results and discussion

5.3.1 Scanning electron microscopy SEM study

SEM images of “cactus” nanotubes grown for 1h are shown in Figure 5.1. “Cactus” knob morphology is observed from the top view image in Figure 5.1(a). The side-view image in Figure 5.1(b) shows that the “cactus” morphology appears only at the top, while the lower part of the nanotubes retain the aligned structure. The length of nanotubes is about 10 μm. The side-view image in Figure 5.1(c) shows that the “cactus” structures are bundled together. Figure 5.1(d) reveals the “cactus” morphology is composed of a large quantity of small nano-sheets with thickness about 1-2 nm. The diameter of the “cactus” part is about 300 nm, while the diameter of the as-grown normal MWNT is about 20-40nm.

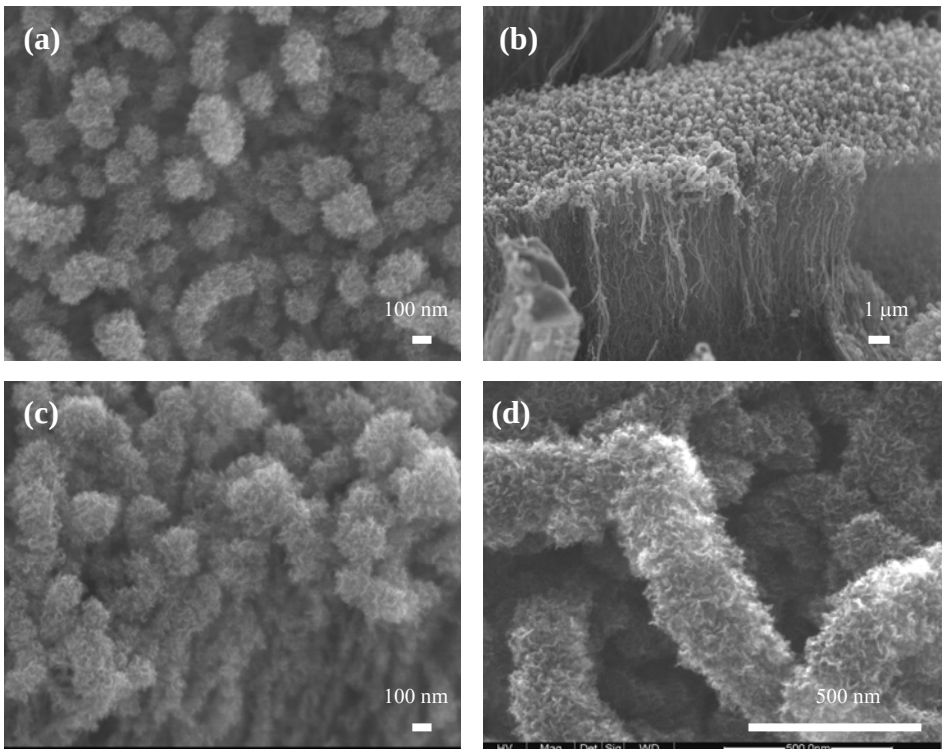

Figure 5.1 (a) SEM image of "cactus" carbon nanotubes from the top view. (b) Side-view picture shows that the cactus structure on the top part of nanotube while the underneath part still remain the aligned structure. (c) Close view of the "cactus" structure on the top part. (d) HRSEM picture of "cactus" nanotubes shows the rough "cactus" surfaces is composed of a large quantity of nano-sheets.

5.3.2 Raman spectroscopy study

Figure 5.2 shows the Raman spectra of "cactus" top-decorated nanotubes and multi-walled nanotubes. In this case, the normal multi-walled carbon nanotube sample was grown on a Si substrate using PECVD under a reactant gas flow (C_2H_2/NH_3, 15sccm/30sccm) at around 700^{o}C for 1h. Previous studies show that for multi-walled CNTs, the G-band corresponds to graphite or ordered carbon, while the D-band indicates disordered or amorphous carbon [11]. In addition, the line width of D-band is related to the amount of amorphous carbon [12].

Based on the curve fitting results, we obtained the ratio ($I_{D/}$ $I_{G)}$ of "cactus" nanotube is about 0.75, while the ratio is only 0.43 for normal multi-walled CNT. In addition, a larger line width of D-band is obtained for "cactus" nanotube. This Raman study indicates a higher amorphous carbon content in "cactus" nanotubes compared with C_2H_2/NH_3 grown multi-walled CNT.

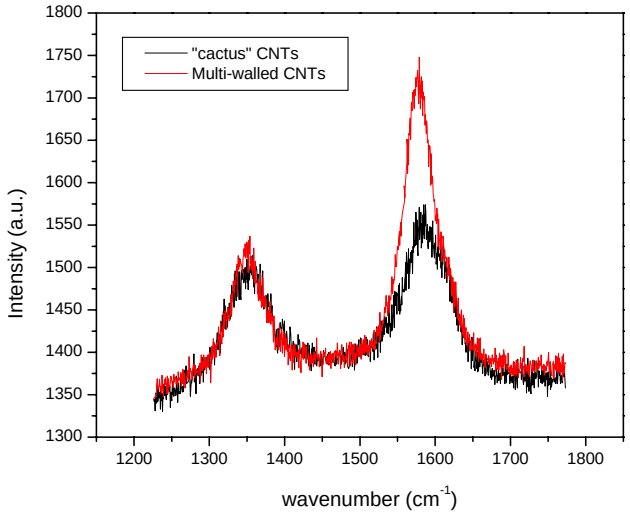

Figure 5.2 Raman spectra for "cactus" nanotube and MWNT grown for 1h.

5.3.3 Transmission electron microscopy TEM study

Figure 5.3(a) shows a typical TEM image of the "cactus" nanotubes lying on the carbon film of a TEM Cu grid. Close-up views at three regions in Figure 5.3(a) are shown in Figure 5.3(b) to (d). Figure 5.3(b) shows the amorphous structure of the top "cactus" part: The layers are not regular and do not have specific orientations. Figure 5.3(c) shows the intermediate part between the top amorphous carbon and the nanotube. It can be seen that some of the graphite layers are broken, and this could be attributed to the strong ion bombardment under plasma during the growth process. These broken layers provide a rich source of dangling bonds for the covalent absorption of activated carbon atoms from the dissociated C_2H_2 precursor. Figure

5.3(d) clearly shows that some outer graphite layers of a nanotube are peeled and only thinner inner layers are left. The electron diffraction pattern further reveals the disordered graphite structure of these “cactus” top-decorated nanotubes. The calculated spacing between different layers of nanotubes is 3.41nm, matching the layer spacing in graphite. The XRD pattern (not shown here) is similar to that of graphite, but the main peak (002) is much weaker and broadened.

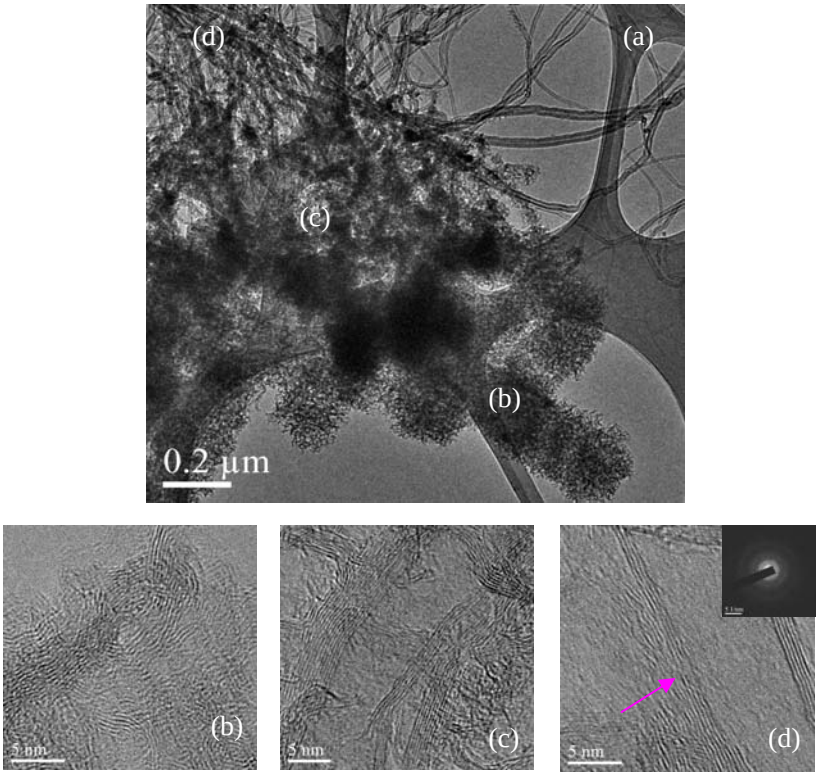

Figure 5.3 (a) Typical HRTEM picture of “cactus” top-decorated nanotube bundles. (b) Amorphous carbon on the top part with no encapsulated catalytic particles. (c) The intermediate part between the amorphous carbon and the lower nanotube body. It shows that the nanotube surface is destroyed and linked with some amorphous carbon. (d) For the lower body of the nanotube, it can be seen that some graphite layers are broken (marked by the

arrow), but the absorption of C atoms become less compared with part (c). ED pattern (Inset) reveals the disordered graphite structure of “cactus” nanotube, the calculated spacing between different layers is 3.41nm, matching the layer spacing in graphite.

5.3.4 X-ray photoelectron spectroscopy (XPS) study

XPS study was carried out to investigate the surface chemical states on the surface of “cactus” and normal multi-walled carbon nanotubes. The contributions of photoelectrons from the diamond-like SP^3 component and graphite SP^2 component can be separated by peak fitting the XPS spectra as shown in Figure 5.4. The C 1s spectra of both samples were fitted with the component peaks at 284.7, 285.2 and 286.5 eV, which correspond to SP^2, SP^3, and C=O or C-O bonds respectively [13, 14]. The SP^3/SP^2 ratios (calculated from the ratio of the areas of the SP^3 and SP^2 peak [15]) for the “cactus” nanotube and MWNTs are 1.59 and 1.13 respectively. Although a higher SP^3 component is obtained for “cactus” nanotubes, no crystalline diamond particle has been observed. Generally, SP^3 C could be bonded to either C or H. A previous study has shown that the hydrogen termination plays an important role in diamond crystallization and growth [16]. In this case, most of the SP^3 carbon bonds are terminated by C atoms due to the lack of H atoms, leading to the formation of amorphous carbon instead of diamond crystalline.

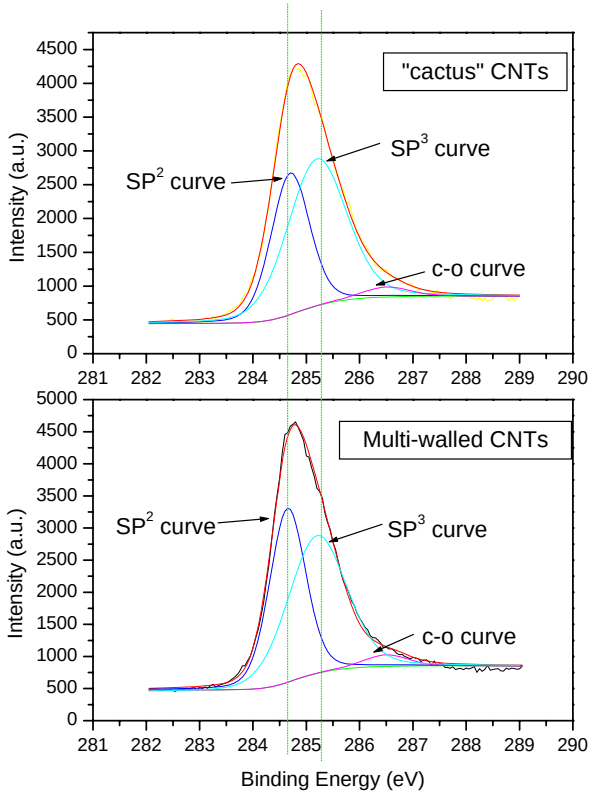

Figure 5.4 XPS spectra of C 1s peak for Multi-walled and "cactus" CNTs. Both samples were fitted with component peaks at 284.7, 285.2 and 286.5eV, which correspond to SP^2, SP^3, and C=O or C-O bond.

5.3.5 Proposed growth mechanism of "cactus" decorated nanotubes

---------- Bottom up root growth and top down strong plasma induced carbon covalent absorption

During the growth process of CNT, the first requirement is the active catalyst. Generally, a small layer of iron oxides will be formed on the catalyst surface. Although no NH_3 or H_2 gas is introduced in the growth, C_2H_2 could still be partially decomposed into carbon and hydrogen ions under plasma irradiation at high temperature (700^oC). Previous studies showed that the absorption process of C_2H_2 molecules on the catalyst surface would produce C-H, C

and H components [9]. The active H ions produced would reduce the iron oxides to form effective catalysts for the nanotube growth. It is well accepted that the growth of carbon nanotubes follows the bottom to up root-growth model [17]. The question is whether the "cactus" appears at the beginning stage or the final stage of the growth process.

In order to resolve this issue, an as-grown normal MWNT sample [SEM image is shown in Figure 5.5(a)] was placed into the PECVD chamber for regrowth according to the growth recipe of "cactus" nanotube for 1h. Similar top-decorated "cactus" morphology is obtained, as shown in Figure 5.5(b). This indicates that the "cactus" does not form bottom-up at the beginning stage. Instead, a top-down strong-plasma induced carbon covalent adsorption mechanism is proposed. Firstly, carbon nanotubes grow following the root growth model. Because of the absence of pretreatment, the decomposition rate of C_2H_2 molecules on the catalytic particle surface is slower, resulting in a higher C_2H_2 concentration in the chamber. Since the plasma can dissociate the hydrocarbon and create a lot of reactive radicals [8], the strength of ion bombardment should be enhanced greatly, destroying the outer graphite layers and producing a lot of dangling bonds, as shown in Figure 5.3(c) and (d). Moreover, the size effect makes the tip more reactive and enhances atomic absorption, deposition, and reconstruction, thus favoring the formation of the amorphous "cactus". At the same time, the carbon nanotubes continue to grow from bottom to up, since the top "cactus" morphology shields most of the ion bombardment from the lower part. Correspondingly, the covalent absorption of carbon atoms would decrease from top to bottom, producing the different diameters observed in the different parts of the nanotubes. The proposed detailed schematic growth process is illustrated in Figure 6. It was also observed that the length of nanotubes is

reduced after the re-growth process [shown in Figure 5.5(b)]. This can be explained by the termination of the catalytic activity during the re-growth process and the strong ion bombardment effect.

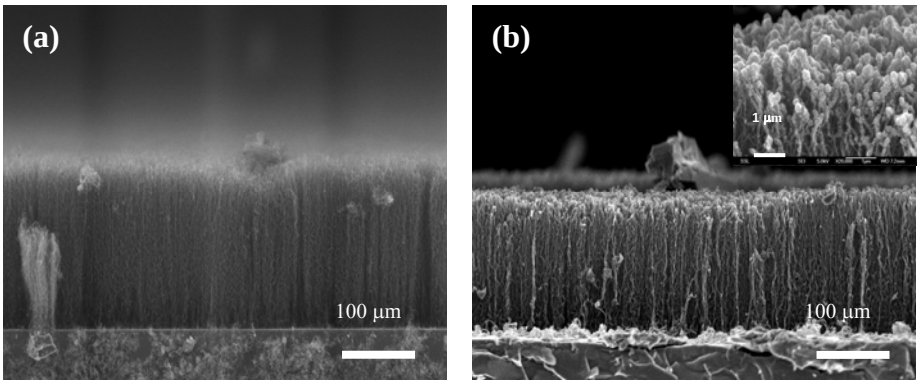

Figure 5.5 (a) is the SEM picture for the as-grown MWNT sample 1(C_2H_2/NH_3, 20 mins), the length of the nanotube is about 20 μm. (b) Re-grown MWNT under C_2H_2 plasma for 1h followed the growth procedure of "cactus" nanotube. "Cactus" morphology is observed on the top part, while the length of re-grown nanotube is slightly shorter than the as-grown one.

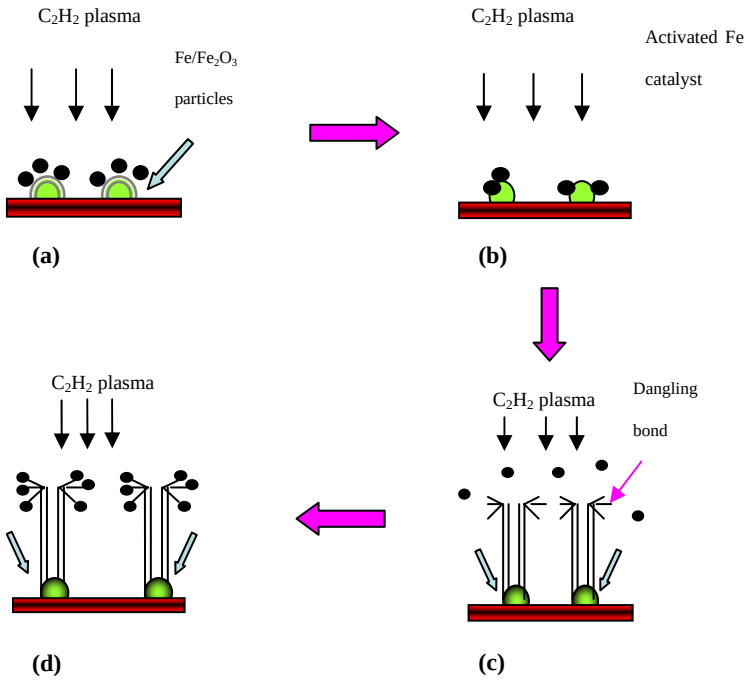

Figure 5.6 (a) C_2H_2 is dissociated under the plasma effect at high temperature (b) Iron oxide layer on the iron particles surface is reduced by the dissociated H atoms (c) nanotubes grow follow the base growth model, and the dangling bonds are produced under the strong plasma (d) covalent absorption of carbon atoms on the top part.

5.3.6 Surface wettability of "cactus" nanotubes

In order to investigate the effect of surface morphology on the surface wettability of CNTs, CA measurements were carried out on the as-grown "cactus" nanotube surface. Previous works of Jiang et al. reported that the nanostructures on a solid surface are important for super-hydrophobicity, which can induce a high CA. [18] However, in our experiments, we did not find any enhancement of surface hydrophobicity for the "cactus" top-decorated CNTs. The average CA is around 148.0 ± 5.0^{o} , which was obtained from the measurements of around 20 droplet images. A typical microscopy image is given in Figure 5.7

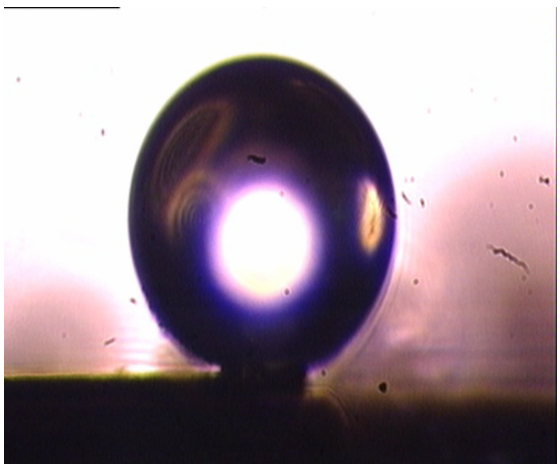

Figure 5.7 A typical microscopic image of a water droplet on "cactus" CNTs.

One possible reason here is that the "cactus" CNTs were grown by using C_2H_2 gas only and the surface chemical composition may be different from the C_2H_2/NH_3 grown MWNTs. More amorphous components were observed based on the Raman studies. Thus, the change of surface morphology is not the dominant factor here.

5.3.7 Third order nonlinearities of "cactus" nanotubes

To evaluate the third order nonlinearities as well as the relaxation dynamic of this "cactus" top decorated carbon nanotubes grown on quartz substrate, open aperture, closed aperture Z scan as well as the degenerate pump probe experiments were performed at 780 nm. The sample with 2.5 μm in thickness is prepared for this optical nonlinearities measurement. Figure 5.8 displays the Z Scan signals. It can be seen from Figure 5.8 (a) that the nonlinear absorption appears as photo-bleaching signal (increased transmittance with increasing laser intensity) while the refractive index is negative in sign. The photo-bleaching is observed in many SWCNTs [19，20] and is believed to due to the state filling effect [18]. It is also observed for MWCNTs [21, 22]. To quantify the observed nonlinear signals, we assume that the nonlinear absorption can be expressed as $\Delta\alpha = \beta I$, and $\Delta n = n_2 I$, where β is the third-order nonlinear absorption coefficient, n_2 the Kerr-type refractive nonlinearity, and I the laser irradiance. Following a Z-scan analytical procedure similar to the one reported in ref [21] to fit the experimental curves, we obtain the β and n_2-values to be $-20 cmGW^{-1}$ and $-3.2\times10^{-4} cm^2 GW^{-1}$, respectively. These two parameters give the value of third-order nonlinear susceptibility $\left|\chi^{(3)}\right|$ of $2.2\times10^{-11} esu$, which is very close to our previous measured result for MWCNTs film [21] despite the different growth condition and outlook of

the two batches of samples. Further Z Scan measurements with different irradiance from 23 $GWcm^{-2}$ to 80 $GWcm^{-2}$ [Figure 5.8(b)] show that both β and n_2 are independent on the laser intensity, indicating the pure third order nonlinearity origin to our Z Scan observations.

For pump probe measurement, the intensity of the pump is varied from 5.4 $GWcm^{-2}$ to 24 $GWcm^{-2}$ while the intensity of the probe beam keeps at 0.15 $GWCm^{-2}$. Figure 5.9 shows the relaxation process of this sample. Two processes can be identified. Fitting the curves with two exponential components, we obtain relaxation time of 260 fs for the faster process and relaxation time of 1ps for the slower process. The faster decay process is believed to be the autocorrelation of the laser pulses while the slower decay process is associated with the electron – phonon interaction as proposed in ref [23]. Figure 5.9 also shows that though the probe signal will increase with the increase of laser beam, the relaxation time remained the same.

To check the effects of the substrate to the measurement results, the substrate was also examined with Z Scan and pump probe experiments. There is no photobleaching signal for it up to the laser intensity of 80 $GWcm^{-2}$, which indicates that the obtained open aperture and pump probe signals are solely from the “cactus” top decorated nanotube film. The closed aperture Z Scan shows that the substrate has a third-order nonlinear refractive index of positive sign, but its magnitude is less than 10% of the n_2 value for the substrate-MWCNT composites so that it can be neglected.

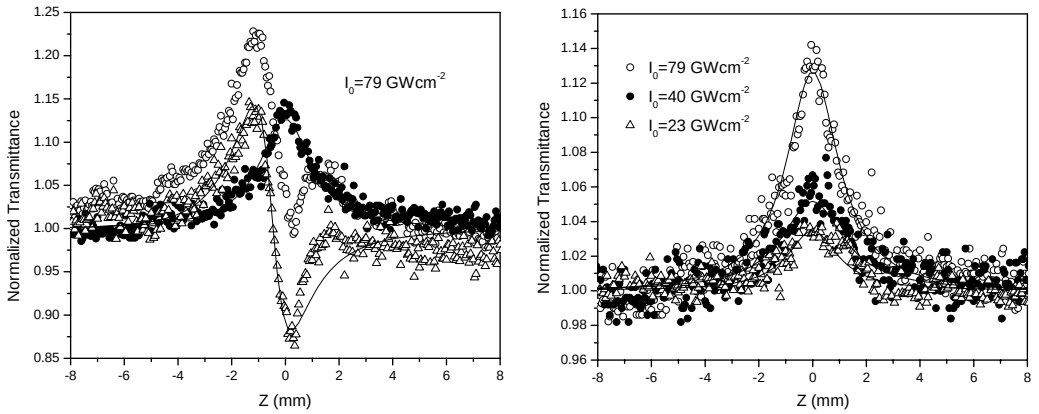

Figure 5.8 (a) At I_0 =79 GWcm^{-2}, open aperture (filled circles), close aperture (open circles) Z Scan results. The open triangles are obtained from close aperture curve divided by open aperture curve. The lines are fitting results. (b) Open aperture Z Scan curves at different laser intensity.

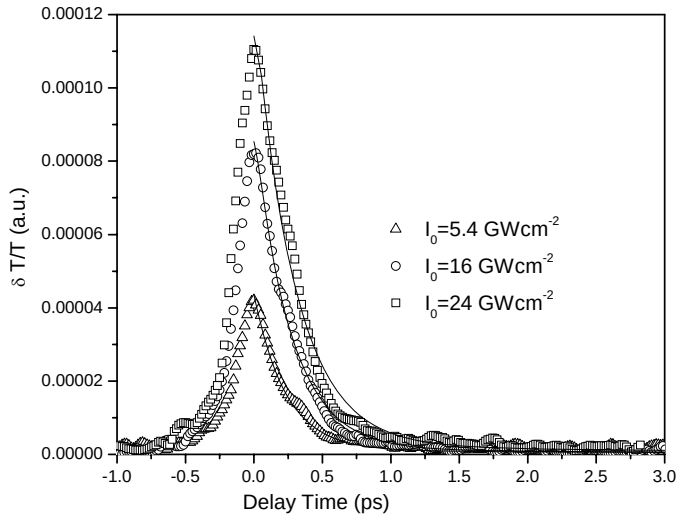

Figure 5.9 Degenerate pump probe signal of "cactus" nanotube at 780 nm.

5.4 Conclusion

The morphology of “cactus” top-decorated aligned carbon nanotubes is reported. HRSEM shows that the top “cactus” is composed of a large quantity of nano-sheets. Raman studies reveal a strong defect component in the “cactus” nanotubes compared with that of C_2H_2/NH_3 grown MWNTs. TEM images show the amorphous carbon nature of the top “cactus” morphology. XPS data reveals a higher SP^3 component, which could be attributed to the bonds between SP^3 C and C atoms. The possible growth mechanism is also investigated. The activity of catalyst is turned on by the dissociation of C_2H_2 on the nanoparticle surface; while the formation of “cactus” morphology is attributed to plasma induced carbon covalent absorption. No enhancement of surface hydrophobicity was observed from CA measurements. The third order nonlinearities are determined with femtosecond Z scan and pump probe techniques at 780 nm. The nonlinear absorption is found to be photo-bleaching type, and the nonlinear absorption coefficient is $-20 cmGW^{-1}$ up to the intensity of 80 GWcm^{-2}. The third-order nonlinear refractive index is $-3.2\times10^{-4} cm^2GW^{-1}$. The nonlinear dynamics shows the relaxation process takes place in about 1.8ps, which is a characteristic relaxation time for MWCNTs.

References:

[1] Dresselhaus MS, Dresselhaus G, Jorio A. Unusual properties and structure of carbon nanotubes. Annu Rev Mater Res 2004;34:247-8.

[2] Dai H. Carbon nanotubes: opportunities and challenges. Surface Science 2002;500:218-41.

[3] Dresselhaus MS, Dresselhaus G, Charlier JC, Hernandez E. Electronic, Thermal and mechanical properties of carbon nanotubes. Phil Trans R Soc lond A 2004;362:2065-98.

[4] Bajpai V, Dai L, Ohashi T. Large-Scale Synthesis of Perpendicularly Aligned Helical Carbon Nanotubes. J Am Chem Soc 2004;126:5070-1.

[5] Lee CJ, park J. Growth model of bamboo-shaped carbon nanotubes by thermal chemical vapor deposition. Appl Phys Lett;77:3397-9.

[6] Trasobares S, Ewels CP, Birrell J, Stephan O, Wei BQ, Carlisle JA, miller D, Keblinski P, Ajayan PM. Carbon Nanotubes with Graphitic Wings. Adv Mater 2004;16:610-3.

[7] Ren ZF, Huang ZP, Xu JW, Wang JH, Bush P, Siegal MP, Provencio PN. Synthesis of large arrays of well-aligned carbon nanotubes on glass. Science 1998;282:1105-7.

[8] Meyyappan M, Delzeit L, Cassell A, Hash D. Carbon nanotube growth by PECVD: a review. Plasma Sources Sci Technol 2003;12:205-16.

[9] Kayastha V, Yap YK, Dimovski S, Gogotsi Y. Controlling dissociative adsorption for effective growth of carbon nanotubes. Appl Phys Lett 2004; 85:3265-7.

[10] Yu XJ, Wilhelmi O, Moser HO, Vidyarai SV, Gao XY, Wee ATS, Nyunt T, Qian HJ, Zheng HW. New soft X-ray facility SINS for surface and nanoscale science at SSLS. Journal

of Electron Spectroscopy and Related Phenomena 2005;144:1031-4.

[11] Nilsson L, Groening O, Emmenegger C, Kuettel O, Schaller E, Schlapbach L, et al. Scanning field emission from patterned carbon nanotube films. Appl Phys Lett 2000;76:2071-3.

[12] Chakrapani N, Curran S, Wei B, Ajayan PM. Spectral finger-printing of structural defects in plasma-treated carbon nanotubes. J Mater Res 2003;18:2515-21.

[13] Filik J, May PW, Pearce SRJ, Wild RK, Hallam KR. XPS and laser Raman analysis of hydrogenated amorphous carbon films. Diamond Relat Mater 2003;12:974-8.

[14] Ago H, Kugler T, Cacialli F, Salaneck WR, Shaffer MSP, Windle AH, Friend RH. Work functions and surface functional groups of Multiwall carbon nanotubes J Phys Chem B 1999;103:8116-21.

[15] Leung TY, Man WF, Lim PK, Chan WC, Gaspari F, Zukotynski S. Determination of the SP^3/ SP^2 ratio of a-C:H by XPS and XAES. J Non-cryst Solids 1999;254:156-160.

[16] Sun L, Gong J, Zhu D, Zhu Z, He S. Diamond nanorods from carbon nanotubes. Adv Mater 2004;16:1849-53.

[17] Fan S, Chapline M, Franklin N, Tombler T, Cassell A, Dai H. Self-oriented regular arrays of carbon nanotubes and their field emission properties. Science 1999;283:512-4.

[18] L. Feng, S. Li, Y. Li, H. Li, L. Zhang, J. Zhai, Y. Song, B. Liu, L. Jiang, D. Zhu, Adv Mater 2002;24:1857-60.

[19] Lauret JS, Voisin C, Cassabois G, Delalande C, Roussignol Ph, Jost O, Capes L. Ultrafast Carrier Dynamics in Single-Wall Carbon Nanotubes. Phys Rev Lett 2003;90:057404-1-057404-4.

[20] Chen YC, Raravikar NR, Schadler LS, Ajayan PM, Zhao YP, Lu TM, Wang GC, Zhang XC. Ultrafast optical switching properties of single-wall carbon nanotube polymer composites at 1.55 mm. Appl Phys Lett 2002;81:975-7.

[21] Elim HI, Ji W, Ma GH, Lim KY, Sow CH, Huan CHA. Ultrafast absorptive and refractive nonlinearities in multiwalled carbon nanotube films. Appl Phys Lett 2004;85:1799-801.

[22] Wang Z, Liu C, Xiang H, Li Z, Gong Q, Qin Y, Guo Z, Zhu D. Ultrafast third-order nonlinear optical response of two soluble multi-wall carbon nanotubes. J Phys D: Appl. Phys 2004;37:1079–82.

[23] Hertel T, Fasel R, Moos G. Charge-carrier dynamics in single-wall carbon nanotube bundles: a time-domain study. Appl Phys A 2002;75:449-65.